Original article

Characterization of time-related changes after experimental bile duct ligation

P. Georgiev[1], W. Jochum[2], S. Heinrich[1], J. H. Jang[1], A. Nocito[1], F. Dahm[1] and P.-A. Clavien[1]

[1]Swiss Hepato-Pancreato-Biliary Centre, Department of Visceral and Transplant Surgery, and [2]Department of Pathology, University Hospital of Zurich, Zurich, Switzerland

Correspondence to: Dr P.-A. Clavien, Department of Visceral and Transplantation Surgery, University Hospital of Zurich, Raemistrasse 100, CH-8091 Zurich, Switzerland (e-mail: clavien@chir.unizh.ch)

Background: **Although bile duct ligation (BDL) in mice is used to study cholestasis, a detailed description of this animal model is lacking. The aim of this study was to define specific phases of acute and chronic injury and repair in the different cellular compartments of the liver.**

Methods: **C57BL/6 mice underwent BDL or sham laparotomy, and serum and liver tissue were analysed between 8 h and 6 weeks later.**

Results: **Biliary infarcts and alanine aminotransferase levels revealed acute hepatocellular injury peaking at days 2–3, paralleled by enhanced transcription of pro-proliferative mediators and followed by a distinct peak of hepatocellular proliferation at day 5. Cholangiocellular proliferation occurred in large bile ducts on days 2–3 and in small bile ducts on day 5. Neutrophil infiltration occurred within 8 h, with neutrophils remaining the predominant immune cell type until day 3. Acute injury was followed by continuous tissue repair, lymphocyte and Kupffer cell infiltration, and accumulation of collagen during the second week. Thereafter, the number of α-smooth muscle actin-positive cells and the expression of transforming growth factor β1, tissue inhibitor of metalloproteinases 1 and procollagen (I) decreased, and liver fibrosis stabilized.**

Conclusion: **BDL elicits dynamic changes in mouse liver. The chronological dissection and quantification of these events identified specific phases of acute and chronic cholestatic liver injury.**

Presented in part to the Annual Meeting of the Swiss Surgical Society, Lugano, Switzerland, June 2006

Paper accepted 27 November 2007

Published online 14 January 2008 in Wiley InterScience (www.bjs.co.uk). **DOI:** 10.1002/bjs.6050

Introduction

Cholestasis is a common pathological condition that can be reproduced in rodents by surgical ligation of the common bile duct. The model of common bile duct ligation (BDL) has been well evaluated and described in rats[1].

Owing to the availability of a variety of genetically modified strains, mice have become a popular model organism for such experiments. Although a detailed description of the morphological and molecular changes following BDL in mice is lacking, this model has been used widely to study cholestatic liver injury[2–7], fibrogenesis[2,3,6,8–10], and the impact of obstructive jaundice on a second hit such as infection[11,12] or hepatic ischaemia[12]. Importantly, the time course of injury and repair in the different cellular compartments of the liver has not been characterized. Therefore, the duration of ligation required to study BDL-related changes in the different cellular compartments of the liver is unknown. For example, a systematic chronological evaluation of hepatocellular injury and proliferation, hepatic inflammation or the development of liver fibrosis following BDL is currently not available. Only the time course of the proliferative response of the biliary epithelium has been described[13,14].

The lack of a detailed description of these time-related changes is reflected in the different time points chosen in previous studies, which often rely on one or two points ranging from 1 day to 12 weeks[3,15–21],

The Editors are satisfied that all authors have contributed significantly to this publication

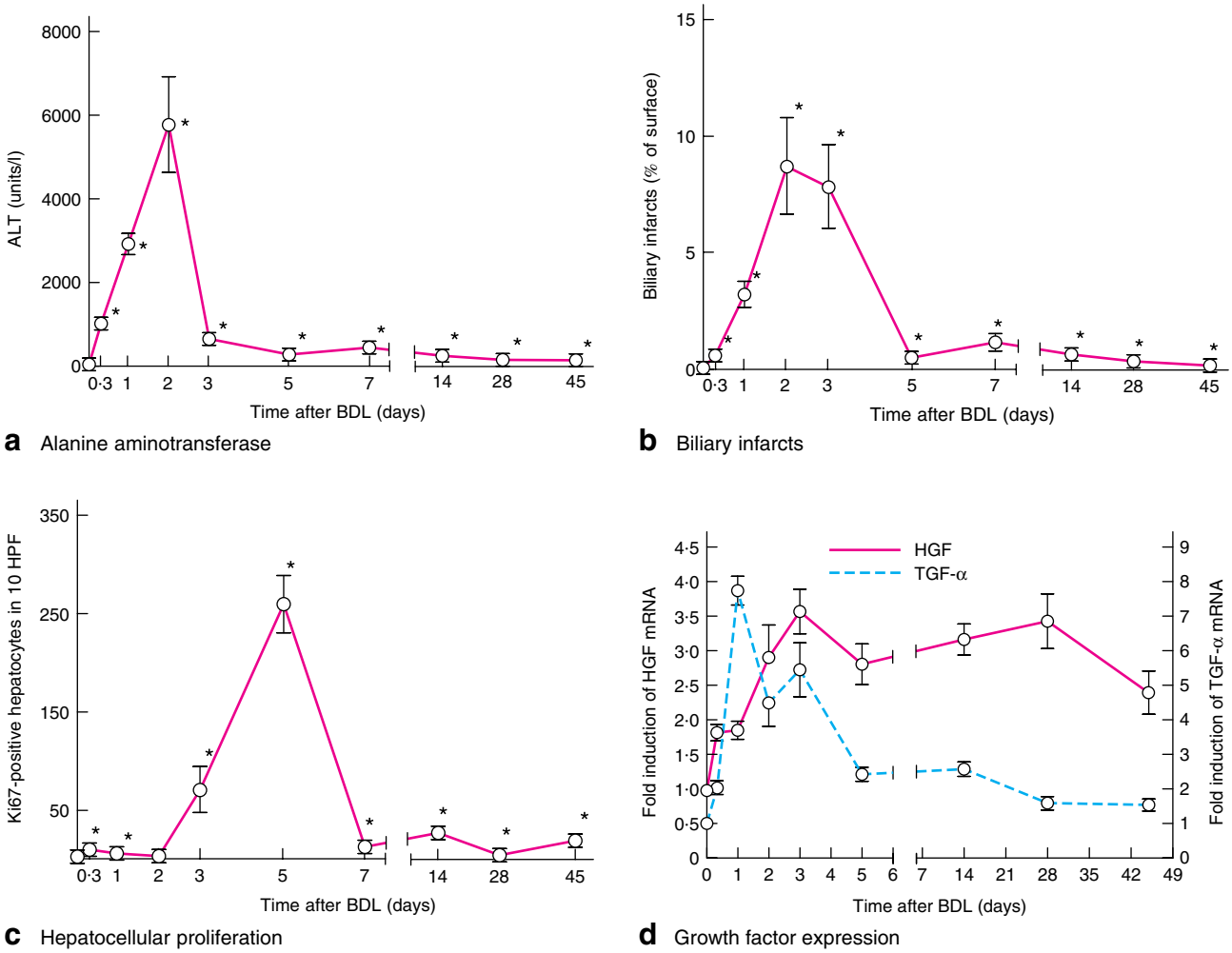

Fig. 1 Hepatocellular injury and proliferation following bile duct ligation (BDL). Liver injury was determined by **a** serum alanine aminotransferase (ALT) levels and **b** histological quantification of biliary infarcts (determined by haematoxylin and eosin staining) in sham animals (time point 0) and after the indicated duration of BDL. **c** Absolute number of Ki67-postive hepatocytes in ten high-power fields (HPF) (400× magnification). **d** Levels of hepatocyte growth factor (HGF) and transforming growth factor (TGF) α mRNA, determined by reverse transcriptase–polymerase chain reaction and expressed as fold induction in comparison to sham-operated controls. Values are mean(s.e.m.) for five to six individual animals per time point. *$P < 0{\cdot}050$ *versus* sham-operated control (two-tailed Mann–Whitney test)

without providing a rationale for the chosen timing. Thus, a detailed evaluation of the various time-related changes after BDL is paramount for the interpretation of available data as well as for the design of future studies.

The present study investigated the impact of BDL in the short (8–48 h), intermediate (3–7 days) and long (14–45 days) term on hepatocellular injury and proliferation, serum markers of cholestasis and cholangiocellular reaction, immune cell infiltration and fibrogenesis.

Methods

Specific pathogen-free male C57BL/6 mice (Harlan Laboratories, Horst, The Netherlands) aged 10–12 weeks were fed on a standard laboratory diet with water and food *ad libitum*, and were kept under controlled environmental conditions with a 12-h light–dark cycle for a minimum of 7 days before surgery. BDL and sham laparotomy were performed as described previously[12].

All animals were checked daily during the first week after the procedure and every other day from week 2 with

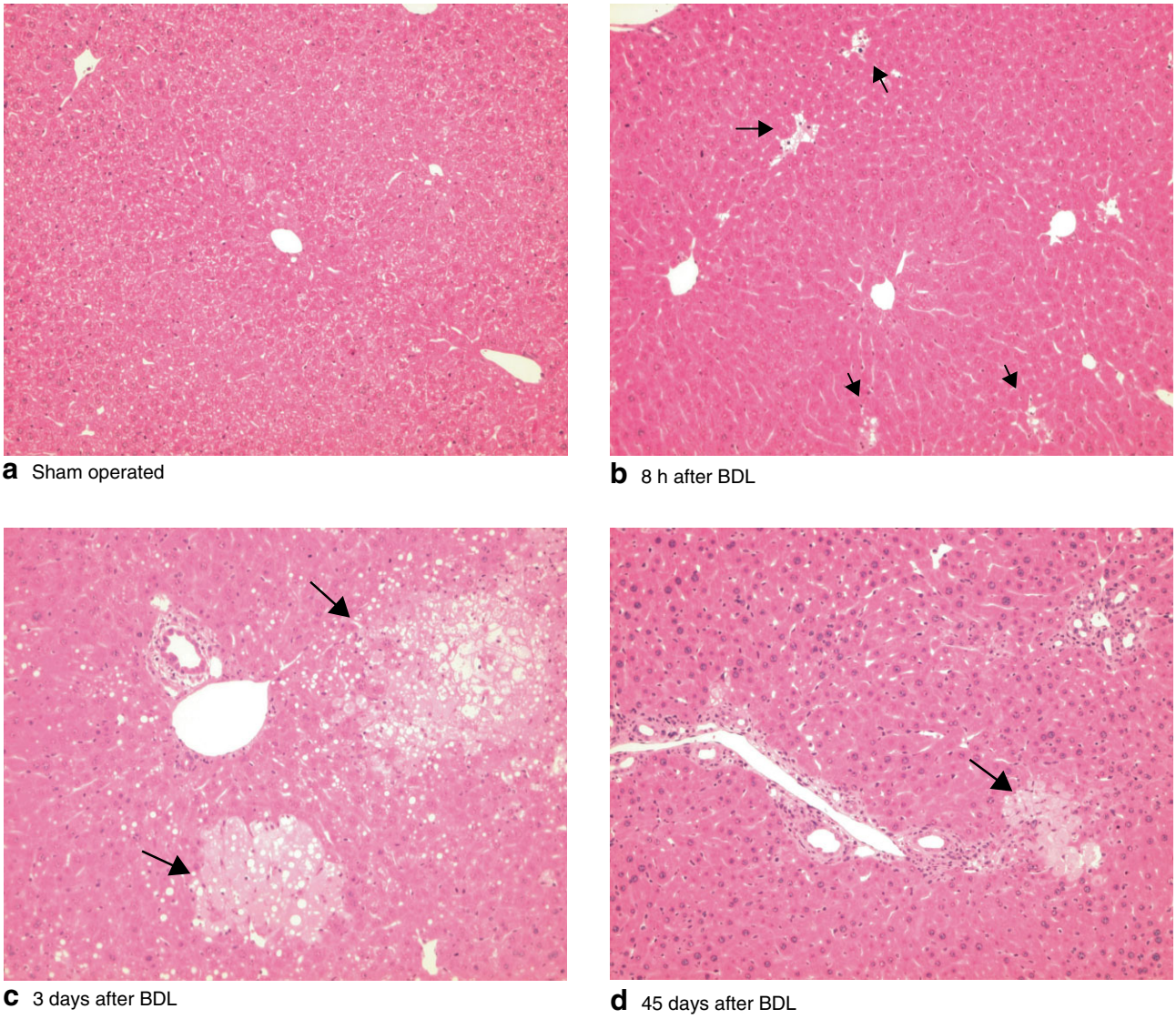

Fig. 2 Representative liver sections from **a** sham-operated controls, and after bile duct ligation (BDL) for **b** 8 h, **c** 3 days and **d** 45 days. Arrows indicate clusters of injured hepatocytes ('biliary infarcts') (haematoxylin and eosin stain, 100× original magnification)

respect to bodyweight, activity and jaundice. Because no data about acute liver injury after BDL were available, analyses were performed daily over the first 3 days and on days 5 and 7. The 2-week time point was chosen based on previous studies that used 2–3 weeks of BDL to study liver fibrogenesis[3,8]. To assess the long-term effects of BDL, analyses were also performed after 4 and 6 weeks. At the indicated time points, blood was drawn from the inferior vena cava. Serum and the left liver lobe were snap-frozen and stored at −80°C until further analysis. The right and the middle liver lobes were immersion-fixed in 4 per cent buffered formalin for histological analysis. All experiments were approved by the Veterinary Office of the Canton of Zurich and carried out according to institutional guidelines.

Measurement of alanine aminotransferase, alkaline phosphatase and bilirubin

Serum levels of alanine aminotransferase (ALT) and alkaline phosphatase were measured using a serum multiple analyser (Ektachem DTSCII; Johnson & Johnson, Rochester, New York, USA). Conjugated and unconjugated bilirubin were measured using the Vitros®

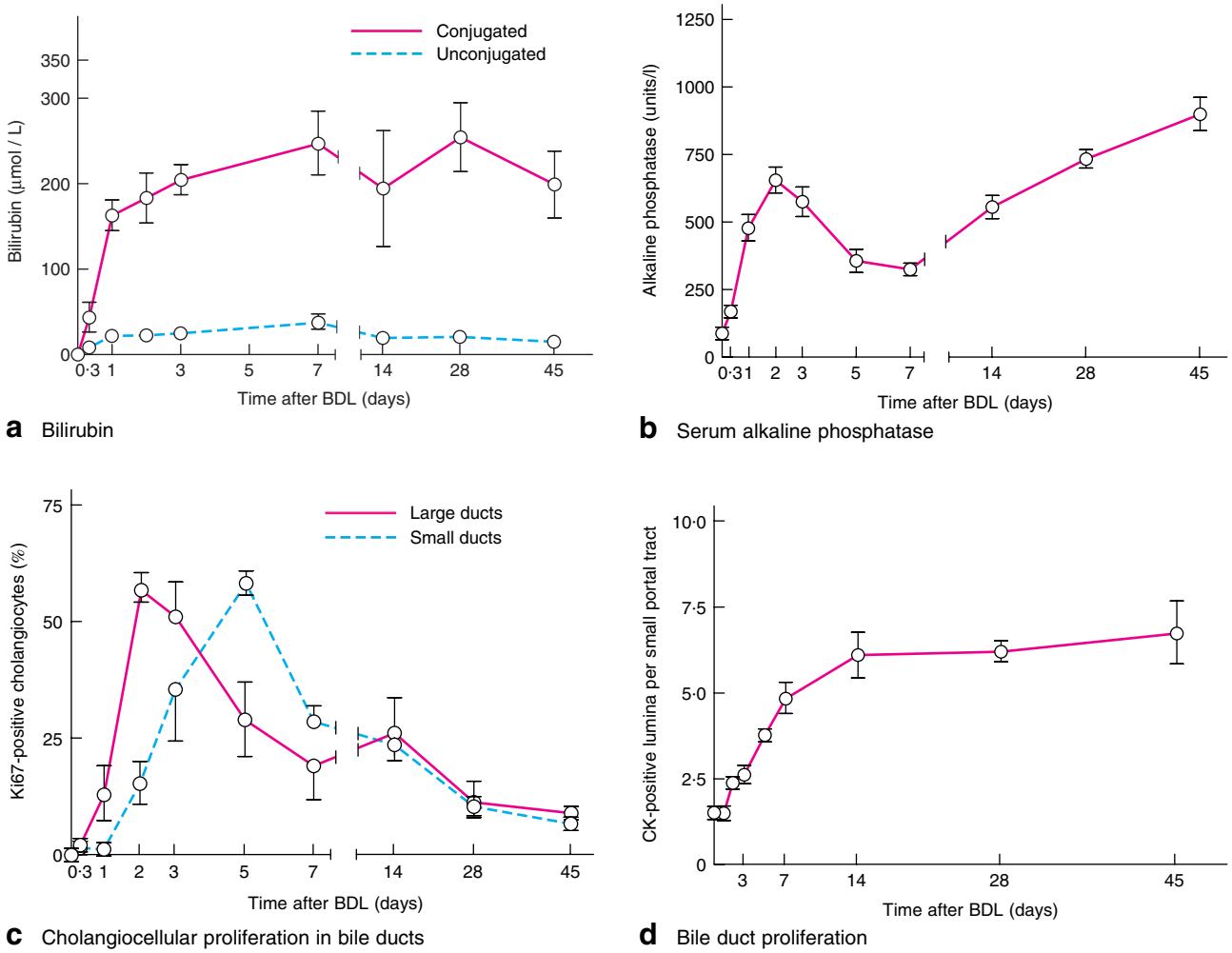

Fig. 3 Serum markers of cholestasis, cholangiocellular proliferation and ductular reaction following bile duct ligation (BDL). Serum levels of **a** conjugated and unconjugated bilirubin and **b** alkaline phosphatase. **c** Proliferation of biliary epithelial cells in small and large bile ducts was determined by staining for Ki67. **d** The ductular reaction was quantified by counting the number of cytokeratin (CK)-positive lumina in small portal tracts. Values are mean(s.e.m.) for five to six individual animals per time point

9500 Chemistry system (Ortho-Clinical Diagnostics, Neckargemünd, Germany).

Histology and immunohistochemistry

Liver tissues were embedded in paraffin, sectioned, and stained with haematoxylin and eosin or Sirius red using standard histological techniques. In addition, slides were immunostained for CD3 (monoclonal rabbit antibody; Neomarkers, Fremont, California, USA), CD45R (B220; monoclonal rat clone RA3-6B2; BD Biosciences Pharmingen, San Diego, California, USA), myeloperoxidase (polyclonal rabbit antibody; Neomarkers), F4/80 (monoclonal rat clone BM8; BMA Biomedicals, Augst, Switzerland), cytokeratin (CK) (polyclonal rabbit antibody; DakoCytomation, Glostrup, Denmark), α-smooth muscle actin (SMA) (monoclonal mouse antihuman, clone 1A4; Dako, Glostrup, Denmark), Ki67 (monoclonal rabbit clone SP6; NeoMarkers) and proliferating cell nuclear antigen (PCNA) (FITC-labelled monoclonal mouse clone PC10; Abcam, Cambridge, UK) using the Ventana Discovery® automated staining system with an iView™ DAB kit (Ventana, Tucson, Arizona, USA). All sections were counterstained with haematoxylin.

For histological quantification of hepatocellular injury ('biliary infarcts'), ten random high-power fields (100× magnification) were evaluated by means of a semiautomatic

image analysis system (Saisam version 4.2.2; Microvision Instruments, Evry, France) and findings expressed as a percentage of liver surface. The percentage of Ki67-positive biliary epithelial cells (BECs) was determined separately for small (fewer than 11 cells per tubular structure) and large (more than 20 cells per tubular structure) bile ducts by counting a minimum of 100 cells per sample. Tangentially sectioned bile ducts, in which one cross-sectional diameter was greater than three times another diameter, were excluded from analysis[13]. The number of Ki67-positive hepatocytes was determined in ten random high-power fields (400× magnification). A semiquantitative evaluation of immune cell infiltration was performed. The percentage of the liver surface positive for Sirius red was determined by analysis of ten random high-power fields (100× magnification) excluding large bile ducts and vessels. The quantification was performed with analySIS[D] software version 5.0 (Soft Imaging System, Münster, Germany). The number of bile ductules per portal field was counted in ten small portal fields per sample. All histological quantifications were first performed as independent semiquantitive analyses by two observers (W.J. and P.G.) followed by quantitative analyses by P.G. as indicated above. The observers who performed the quantitative histological analyses were blinded with respect to treatment group (BDL *versus* sham) and duration of ligation.

Quantitative real-time polymerase chain reaction

For reverse transcriptase–polymerase chain reaction (RT–PCR) total RNA was extracted from 50 mg liver tissue using TRIzol® reagent (Invitrogen, Paisley, UK). Some 5 μg RNA was reverse transcribed using the ThermoScript™ (Invitrogen) RT–PCR System. Quantitative real-time PCR amplification and data analysis were performed using an ABI Prism® 7000 Sequence Detection System (PE Applied Biosystems, Rotkreuz, Switzerland). TaqMan® gene expression assays (PE Applied Biosystems) for transforming growth factor (TGF) β1 (assay ID Mm00441724_m1), procollagen (I) α1 (assay ID Mm00801666_g1), hepatocyte growth factor (HGF) (assay ID Mm01135190_m1), TGF-α (assay ID Mm00446231_m1) and tissue inhibitor of metalloproteinases (TIMP) 1 (assay ID Mm00441818_m1) were used to quantify mRNA expression of the respective genes. The housekeeping gene 18S rRNA (TaqMan® ribosomal RNA control reagents; PE Applied Biosystems) was used for normalization.

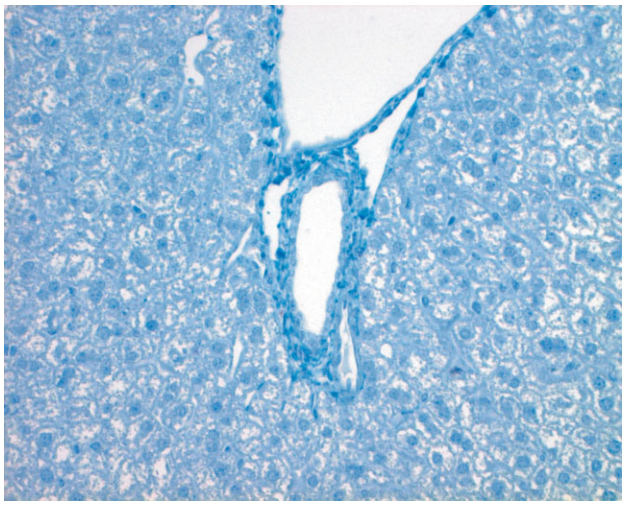

a Sham operated

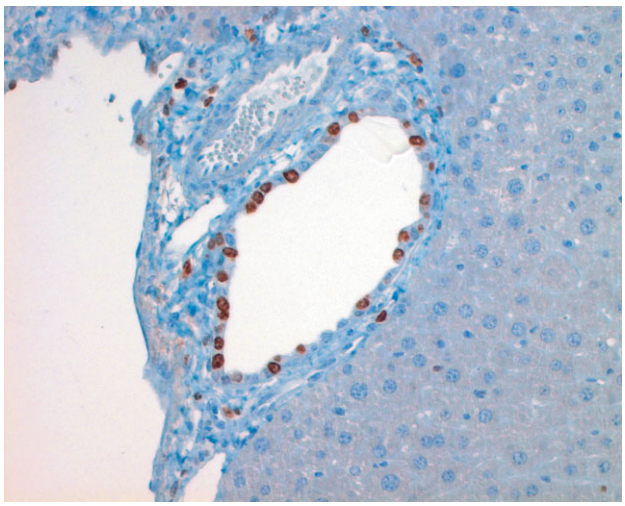

b 2 days after BDL

Fig. 4 Representative liver sections immunostained for Ki67 from **a** sham-operated controls and **b** 2 days after bile duct ligation (BDL), showing cholangiocellular proliferation in large bile ducts (250× original magnification)

Statistical analysis

Values are expressed as mean(s.e.m.). Statistical significance was determined by the two-tailed Mann–Whitney test. $P < 0{\cdot}050$ was considered to indicate statistical significance.

Results

Impact of bile duct ligation on survival, bodyweight, activity and jaundice

No significant changes in evaluated variables were identified between time points for sham-operated animals.

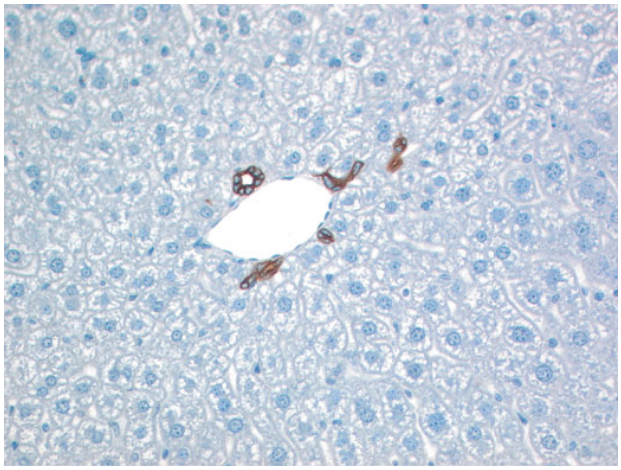

a Sham operated

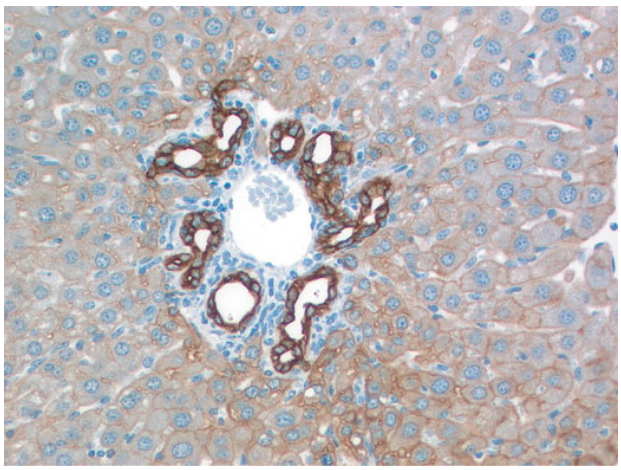

b 14 days after BDL

Fig. 5 Representative liver sections immunostained for cytokeratin from **a** sham-operated controls and **b** 14 days after bile duct ligation (BDL) (160× original magnification)

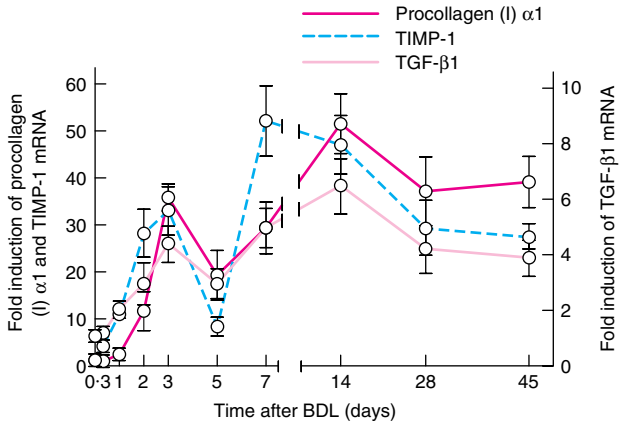

a Markers of liver fibrosis

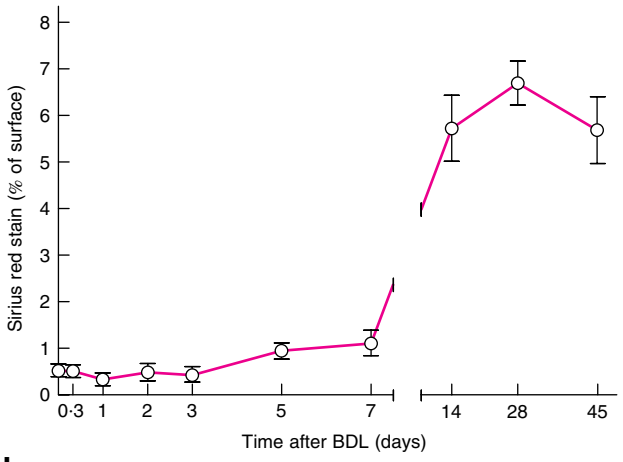

b Quantification of liver fibrosis

Fig. 6 Markers of liver fibrosis during bile duct ligation (BDL). **a** Levels of mRNA for procollagen (I) α1, tissue inhibitor of metalloproteinases (TIMP) 1 and transforming growth factor (TGF) β1, determined by reverse transcriptase–polymerase chain reaction and expressed as fold induction in comparison to sham-operated controls. **b** Percentage of liver surface stained with Sirius red. Values are mean(s.e.m.) for five to six individual animals per time point

To ease the readability of the graphs, data from sham animals were pooled and set as time point 0 for all endpoints.

All sham-operated animals survived for up to 6 weeks whereas nine of 63 mice in the BDL group became moribund and were killed before the planned time point. Significant weight loss was observed during the first 3 days after BDL (18(1) per cent *versus* 3(0·3) per cent in sham-operated animals) but bodyweight stabilized thereafter. The activity of sham-operated animals remained unaltered, whereas mice subjected to BDL displayed reduced activity during the first 2 days but regained normal activity after day 3. Jaundiced skin was apparent in all animals by day 1 after BDL.

Hepatocellular injury

To investigate the course of hepatocellular injury following BDL, serum levels of ALT were determined and a histological quantification of biliary infarcts was performed. ALT increased rapidly after BDL, peaking at day 2. After this acute ALT release, serum levels remained raised until 45 days after BDL (*Fig. 1a*). Biliary infarcts, defined as clusters of injured hepatocytes, were detected 8 h after BDL and increased in size and number at days 2–3. Paralleling ALT, they almost completely disappeared by day 5 and few biliary

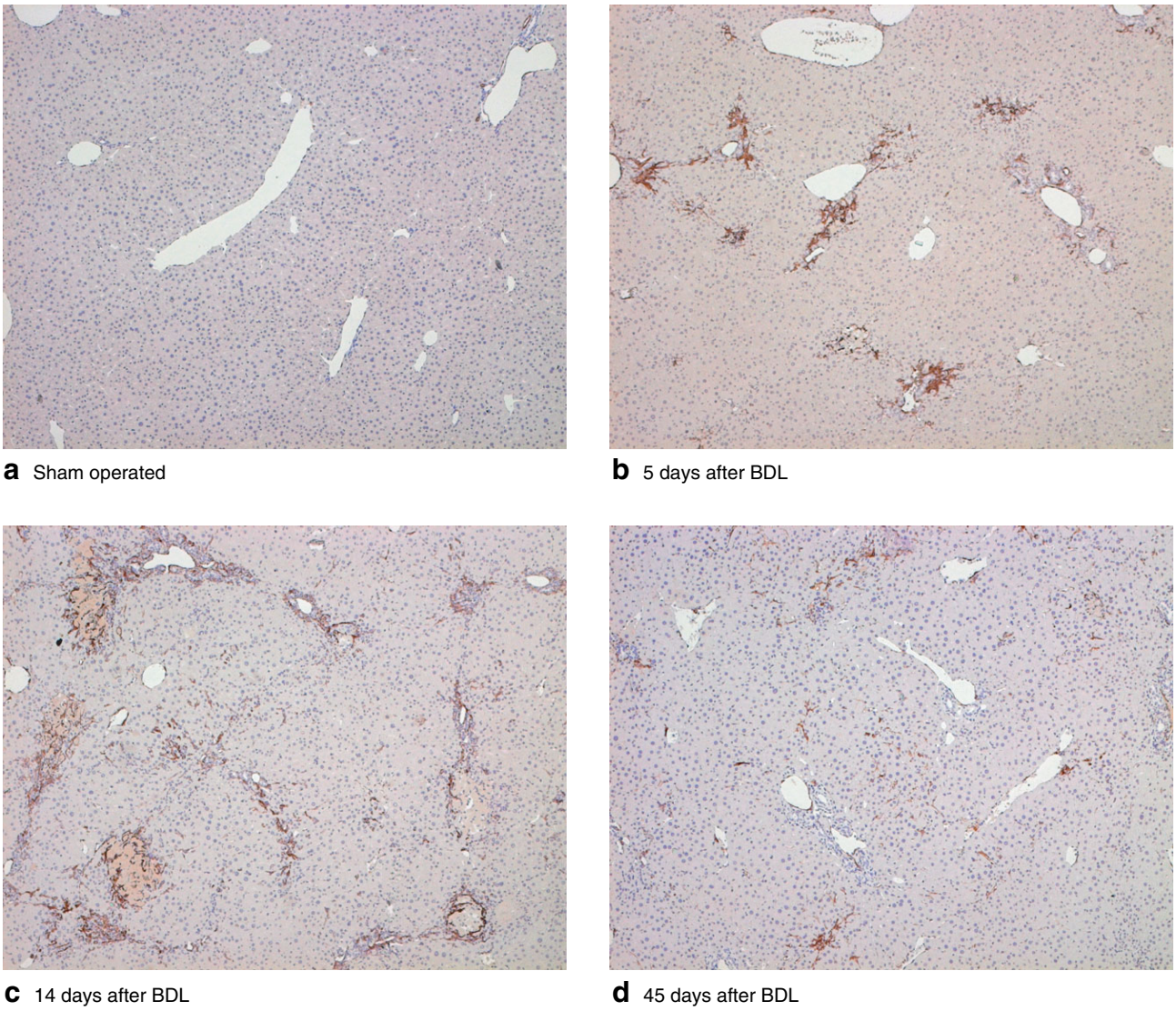

Fig. 7 Representative liver sections immunostained for α-smooth muscle actin from **a** sham-operated controls, and after bile duct ligation (BDL) for **b** 5 days, **c** 14 days and **d** 45 days (50× original magnification)

infarcts were detectable at later time points (*Figs 1b* and *2*).

Hepatocellular proliferation

To study the proliferative response of hepatocytes after BDL the number of Ki67-positive hepatocytes was determined (*Fig. 1c*). To confirm these results, immunohistochemical staining for PCNA, a second established marker for hepatocyte proliferation, was performed. Semiquantitative analysis of PCNA-positive hepatocytes revealed similar results with respect to the distribution and number of labelled hepatocytes (data not shown).

To determine whether BDL induces the expression of proliferative mediators, gene expression levels of two key mediators of hepatocellular regeneration, HGF and TGF-α, were measured by quantitative RT–PCR. Transcript levels of both HGF and TGF-α increased rapidly after BDL with initial peaks 1 day (TGF-α) or 3 days (HGF) after BDL (*Fig. 1d*). Together, these data indicate that BDL rapidly led to hepatocellular injury and gene activation, initiating a regenerative response which culminated in a distinct peak of hepatocellular proliferation at day 5.

Serum markers of cholestasis

BDL results in an increase in serum markers of cholestasis such as bilirubin and alkaline phosphatase. Conjugated and unconjugated bilirubin levels increased steadily and in parallel until day 7 and remained high thereafter (*Fig 3a*).

Alkaline phosphatate production is induced after BDL in rats[22] and its release from the canalicular membrane of hepatocytes is modulated by bile acids[23]. Serum levels of alkaline phosphatase showed a biphasic course, peaking on day 2 and then increasing steadily from day 7 onwards (*Fig. 3b*).

Cholangiocellular proliferation and ductular reaction

As in hepatocytes, BDL induces proliferation of BECs. Using a technique adapted from that of Liu and colleagues[13], Ki67-positive BECs were quantified in small (fewer than 11 cells) and large (more than 20 cells) bile ducts and expressed as a percentage of all BECs. A first peak of Ki67-positive BECs occurred at days 2 and 3 in large bile ducts, followed by a second peak in small bile ducts at day 5 after BDL (*Figs 3c* and *4*). Low-level proliferative activity of BECs was maintained in both small and large bile ducts until day 45, as noted in hepatocytes.

Bile duct obstruction also leads to increased numbers of bile ducts in small portal tracts, a response termed 'ductular reaction' or 'bile duct proliferation'. This characteristic morphological response was evaluated by immunostaining with a CK antibody (*Fig. 5*). The number of CK-positive bile ducts per portal field began to rise by day 2 after BDL and steadily increased until day 14, with no further increase thereafter (*Fig. 3d*).

Inflammatory response in the liver

Histological examination of livers after BDL revealed large numbers of inflammatory cells that initially infiltrated mainly into and around biliary infarcts, and then shifted towards the portal tracts from day 5 onwards. To differentiate the type of infiltrating immune cells during the acute and chronic phase after BDL, immunohistochemical staining for neutrophils, Kupffer cells, T cells and B cells was performed. Immune cell infiltration occurred within 8 h after BDL. Until day 3, neutrophils represented the predominant infiltrating cell type, mainly in areas of injured hepatocytes and in surrounding sinusoids (not shown). A prominent increase in Kupffer cells was observed at 2 weeks, whereas no obvious changes in Kupffer cell number and distribution were apparent at the early time points. From day 5 onwards, increasing numbers of T cells and a slight increase in B cells were detected in portal tracts. T cells were found until 6 weeks after BDL, whereas B cells had disappeared from the portal tracts at the late time points (not shown).

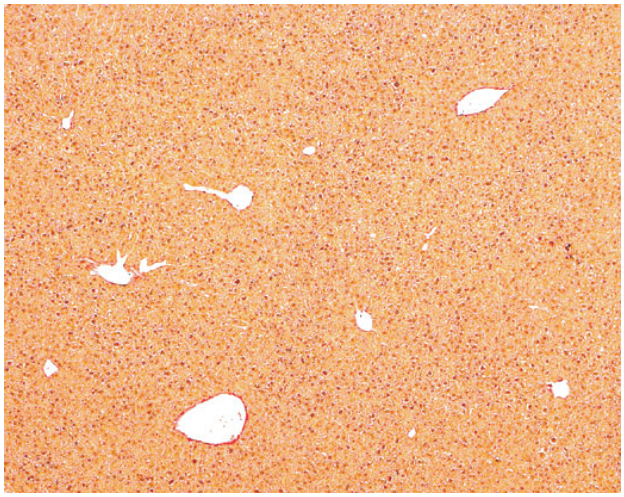

a Sham operated

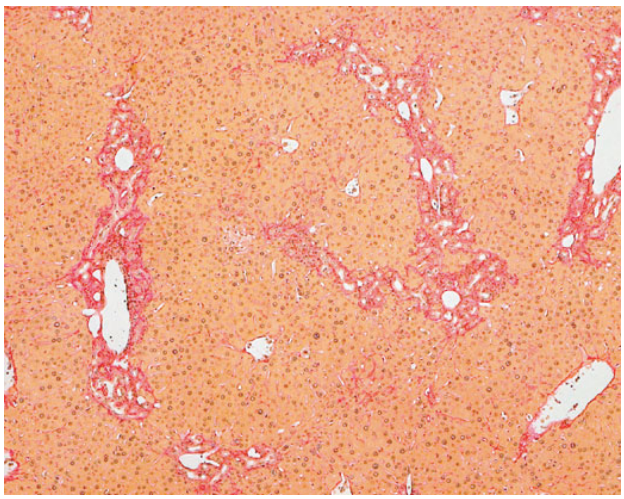

b 45 days after BDL

Fig. 8 Representative Sirius red-stained liver sections from **a** sham-operated controls and **b** 45 days after bile duct ligation (BDL) (50× original magnification)

Development of liver fibrosis

Quantitative RT–PCR was used to determine the time course of three markers of liver fibrosis, TIMP-1, TGF-β1 and type I collagen. An initial peak at day 3 after BDL was followed by lower transcript levels at day 5 and a second peak at day 7 (TIMP-1) or day 14 (TGF-β1 and type I collagen) (*Fig. 6a*).

To analyse activated hepatic stellate cells, an immunohistochemical analysis for α-SMA was performed. α-SMA-positive cells were first detectable around biliary infarcts at

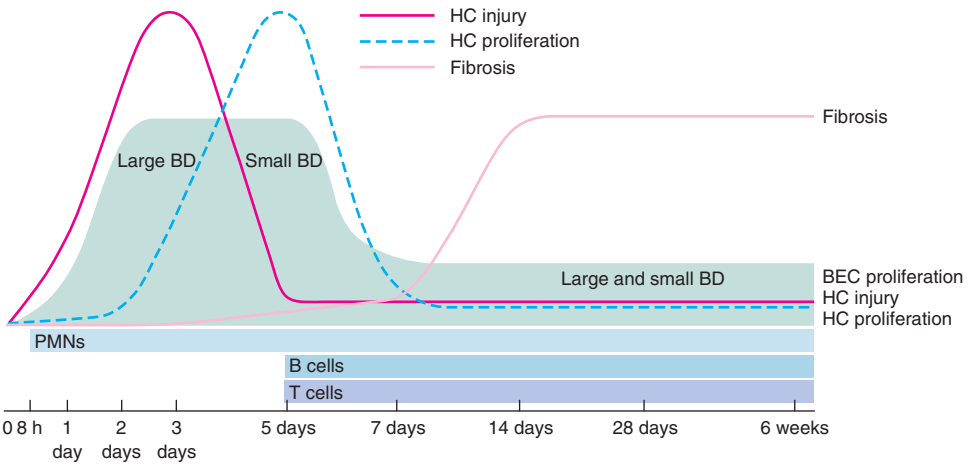

Fig. 9 Overview of dynamic changes following bile duct ligation in mice. BD, bile duct; BEC, biliary epithelial cell; HC, hepatocyte; PMN, polymorphonuclear leucocyte

day 3. From day 5 onwards, they were predominantly found in portal tracts and around resolving biliary infarcts, forming partial 'bridges' between portal tracts. Twenty-eight and 45 days after BDL, however, the number of α-SMA-positive cells decreased and the distribution shifted from a dense interportal or 'bridging' pattern towards a reticular pattern in the lobular parenchyma (*Fig.* 7). In accordance with these findings, accumulation of collagen was observed until day 14, with no further increase thereafter as determined by quantification of the Sirius red-positive liver surface (*Figs 6b* and *8*).

Discussion

Well characterized animal models of human diseases are fundamental for the analysis of pathogenetic mechanisms and the development of new treatment strategies. The main findings of this investigation of time-related changes in liver after BDL in a mouse model of cholestasis are summarized in *Fig. 9*.

Serum levels of ALT and biliary infarcts increased after BDL, peaking at days 2 and 3 respectively. Several groups have assessed hepatocellular injury on day 3 after BDL[2–4], whereas others have also determined hepatocyte injury after 7 days[5] or 14 days[6]. The present data indicate that day 3 after BDL is a valid time point for histological quantification, but ALT should be measured after 24–48 h to determine the degree of acute cholestatic liver injury.

Following acute or chronic tissue loss, hepatocytes mount a proliferative response. BDL induced a distinct peak of hepatocellular proliferation at day 5, approximately 48 h after the peak of histologically detectable hepatocellular injury. These findings indicate that hepatocyte proliferation after acute cholestatic liver damage follows a similar time course to that after 70 per cent hepatectomy, with a peak 36–48 h after tissue loss[24,25]. After the initial peak on day 5, continuous proliferation was observed at a low level. The proportion of continuously proliferating hepatocytes is in the range of 1–3 per cent[5,14,26,27]. The present data suggest that hepatocellular proliferation in response to acute cholestatic liver injury can best be evaluated in the first week after BDL, whereas day 14 (or later) is appropriate for the evaluation of hepatocellular proliferation during chronic cholestasis.

Serum levels of alkaline phosphatase and bilirubin are classical markers of obstructive cholestasis in the clinical setting[28]. Raised serum levels of alkaline phosphatase are due to *de novo* synthesis in the liver[22]. Interestingly, serum levels of alkaline phosphatase were found not to increase progressively after BDL. A first peak during the acute phase was followed by decreasing levels from day 3 to day 7, indicating that the acute injury triggers a massive production and release of this enzyme. The steady increase in alkaline phosphatase levels thereafter was presumably due to persistently raised bile acid levels[23].

BDL induced BEC proliferation in both small and large bile ducts. Proliferation of BECs in large ducts preceded the peak proliferative activity in small bile ducts by 3 days, indicative of a proliferative wave from extrahepatic to intrahepatic bile ducts during the acute and subacute phase of obstructive cholestasis. After this differential proliferative response from large to small bile ducts, cell proliferation reached a steady state in the BEC compartment by day 14. Experiments investigating BEC proliferation during the early phase of BDL need to take the differential courses of small and large bile ducts into account.

Inflammation is a fundamental component of acute and chronic cholestatic liver injury. Neutrophils contribute to cholestatic liver injury after BDL for 3 days[29,30], whereas Kupffer cells are believed to abrogate acute cholestatic liver injury through the release of interleukin 6[31]. Little attention has been paid to the role of lymphocytes, which are known to modulate liver fibrosis in other models of liver disease[32,33]. The histological analysis indicated that both B and T cells were present in the portal tracts of mice after day 5 of BDL. Interestingly, both cell types accumulated mainly during the phase of collagen deposition and thus may also be involved in the process of fibrogenesis following BDL. The exact role of B and T cells after BDL remains to be investigated.

It is well established that BDL induces fibrogenesis in the liver. Transcript levels for type I collagen, TIMP-1, and TGF-β1 increased rapidly after BDL, and α-SMA-positive cells appeared at day 3. Collagen deposition was visible at the end of the first week. Activation of the fibrogenetic process during the first week presumably resulted in further collagen deposition by α-SMA-positive cells during the second week. Thereafter, transcript levels for collagen, TIMP-1 and TGF-β1 decreased in parallel with the number of periportal α-SMA-positive cells and collagen was not deposited any further. These findings are in contrast to descriptions of the rat model, in which fibrosis is progressive and liver cirrhosis can develop within 2 weeks after BDL[34]. The mechanisms underlying this interspecies difference are unknown. Although BDL in mice did not result in liver cirrhosis, it is suitable for the study of liver fibrosis provided that the limitations of the model are taken into account.

Male inbred C57BL/6 mice were studied because a wide range of genetically modified mouse strains are available on this genetic background. During pilot studies BDL was also performed in female C57BL/6 mice. As a large number of female mice became moribund and had to be killed soon after BDL, it appears that male mice are more suited to this type of experiment.

BDL in mice induces dynamic changes in the liver. The first week after BDL reflects the acute cholestatic injury with consequent reparative reactions, followed by a phase of chronic injury resulting in liver fibrosis. The description of these dynamic changes may provide a basis for the design of future studies based on this mouse model.

Acknowledgements

P.G. and W.J. contributed equally to this manuscript. The authors thank Dr J. Flückiger (Logolab AG, Zürich, Switzerland) and Polymed AG (Glattbrugg, Switzerland) for the measurement of bilirubin, and M. Bawohl, K. Mahler, S. Behnke and U. Ungethüm for excellent technical assistance. This study was supported by the Hartmann Müller Foundation (to P.G.), the Swiss National Foundation (grant no. 32-61411 to P.A.C.) and the Gebert Ruf Foundation (to W.J.). P.G. is a participant in the MD/PhD programme at the University of Zurich.

References

1 Johnstone JM, Lee EG. A quantitative assessment of the structural changes in the rat's liver following obstruction of the common bile duct. *Br J Exp Pathol* 1976; **57**: 85–94.
2 Miyoshi H, Rust C, Roberts PJ, Burgart LJ, Gores GJ. Hepatocyte apoptosis after bile duct ligation in the mouse involves Fas. *Gastroenterology* 1999; **117**: 669–677.
3 Canbay A, Higuchi H, Bronk SF, Taniai M, Sebo TJ, Gores GJ *et al*. Fas enhances fibrogenesis in the bile duct ligated mouse: a link between apoptosis and fibrosis. *Gastroenterology* 2002; **123**: 1323–1330.
4 Gujral JS, Liu J, Farhood A, Jaeschke H. Reduced oncotic necrosis in Fas receptor-deficient C57BL/6J-lpr mice after bile duct ligation. *Hepatology* 2004; **40**: 998–1007.
5 Wang H, Vohra BP, Zhang Y, Heuckeroth RO. Transcriptional profiling after bile duct ligation identifies PAI-1 as a contributor to cholestatic injury in mice. *Hepatology* 2005; **42**: 1099–1108.
6 Bergheim I, Guo L, Davis MA, Duveau I, Arteel GE. Critical role of plasminogen activator inhibitor-1 in cholestatic liver injury and fibrosis. *J Pharmacol Exp Ther* 2006; **316**: 592–600.
7 Fickert P, Zollner G, Fuchsbichler A, Stumptner C, Weiglein AH, Lammert F *et al*. Ursodeoxycholic acid aggravates bile infarcts in bile duct-ligated and Mdr2 knockout mice via disruption of cholangioles. *Gastroenterology* 2002; **123**: 1238–1251.
8 Bataller R, Schwabe RF, Choi YH, Yang L, Paik YH, Lindquist J *et al*. NADPH oxidase signal transduces angiotensin II in hepatic stellate cells and is critical in hepatic fibrosis. *J Clin Invest* 2003; **112**: 1383–1394.
9 Yang L, Bataller R, Dulyx J, Coffman TM, Gines P, Rippe RA *et al*. Attenuated hepatic inflammation and fibrosis in angiotensin type 1a receptor deficient mice. *J Hepatol* 2005; **43**: 317–323.
10 Isayama F, Hines IN, Kremer M, Milton RJ, Byrd CL, Perry AW *et al*. LPS signaling enhances hepatic fibrogenesis caused by experimental cholestasis in mice. *Am J Physiol Gastrointest Liver Physiol* 2006; **290**: G1318–G1328.
11 Abe T, Arai T, Ogawa A, Hiromatsu T, Matsuda A, Matsuguchi T *et al*. Kupffer cell-derived interleukin 10 is responsible for impaired bacterial clearance in bile duct-ligated mice. *Hepatology* 2004; **40**: 414–423.
12 Georgiev P, Navarini AA, Eloranta JJ, Lang KS, Kullak-Ublick GA, Nocito A *et al*. Cholestasis protects the liver from ischaemic injury and post-ischaemic inflammation in the mouse. *Gut* 2007; **56**: 121–128.
13 Liu Z, Sakamoto T, Ezure T, Yokomuro S, Murase N, Michalopoulos G *et al*. Interleukin-6, hepatocyte growth factor, and their receptors in biliary epithelial cells during a type I ductular reaction in mice: interactions between the

periductal inflammatory and stromal cells and the biliary epithelium. *Hepatology* 1998; **28**: 1260–1268.
14 Ezure T, Sakamoto T, Tsuji H, Lunz JG III, Murase N, Fung JJ *et al*. The development and compensation of biliary cirrhosis in interleukin-6-deficient mice. *Am J Pathol* 2000; **156**: 1627–1639.
15 Wang M, Tan Y, Costa RH, Holterman AX. *In vivo* regulation of murine CYP7A1 by HNF-6: a novel mechanism for diminished CYP7A1 expression in biliary obstruction. *Hepatology* 2004; **40**: 600–608.
16 Canbay A, Guicciardi ME, Higuchi H, Feldstein A, Bronk SF, Rydzewski R *et al*. Cathepsin B inactivation attenuates hepatic injury and fibrosis during cholestasis. *J Clin Invest* 2003; **112**: 152–159.
17 Higuchi H, Bronk SF, Taniai M, Canbay A, Gores GJ. Cholestasis increases tumor necrosis factor-related apoptotis-inducing ligand (TRAIL)-R2/DR5 expression and sensitizes the liver to TRAIL-mediated cytotoxicity. *J Pharmacol Exp Ther* 2002; **303**: 461–467.
18 Higuchi H, Miyoshi H, Bronk SF, Zhang H, Dean N, Gores GJ. Bid antisense attenuates bile acid-induced apoptosis and cholestatic liver injury. *J Pharmacol Exp Ther* 2001; **299**: 866–873.
19 Lunz JG III, Tsuji H, Nozaki I, Murase N, Demetris AJ. An inhibitor of cyclin-dependent kinase, stress-induced p21Waf-1/Cip-1, mediates hepatocyte mito-inhibition during the evolution of cirrhosis. *Hepatology* 2005; **41**: 1262–1271.
20 Fickert P, Trauner M, Fuchsbichler A, Stumptner C, Zatloukal K, Denk H. Bile acid-induced Mallory body formation in drug-primed mouse liver. *Am J Pathol* 2002; **161**: 2019–2026.
21 Magness ST, Bataller R, Yang L, Brenner DA. A dual reporter gene transgenic mouse demonstrates heterogeneity in hepatic fibrogenic cell populations. *Hepatology* 2004; **40**: 1151–1159.
22 Kaplan MM, Righetti A. Induction of rat liver alkaline phosphatase: the mechanism of the serum elevation in bile duct obstruction. *J Clin Invest* 1970; **49**: 508–516.
23 Hatoff DE, Hardison WG. Bile acid-dependent secretion of alkaline phosphatase in rat bile. *Hepatology* 1982; **2**: 433–439.
24 Seki E, Tsutsui H, Iimuro Y, Naka T, Son G, Akira S *et al*. Contribution of Toll-like receptor/myeloid differentiation factor 88 signaling to murine liver regeneration. *Hepatology* 2005; **41**: 443–450.
25 Huang W, Ma K, Zhang J, Qatanani M, Cuvillier J, Liv J *et al*. Nuclear receptor-dependent bile acid signaling is required for normal liver regeneration. *Science* 2006; **312**: 233–236.
26 Liu Z, Sakamoto T, Yokomuro S, Ezure T, Subbotin V, Murase N *et al*. Acute obstructive cholangiopathy in interleukin-6 deficient mice: compensation by leukemia inhibitory factor (LIF) suggests importance of gp-130 signaling in the ductular reaction. *Liver* 2000; **20**: 114–124.
27 Bird MA, Lange PA, Schrum LW, Grisham JW, Rippe RA, Behrns KE. Cholestasis induces murine hepatocyte apoptosis and DNA synthesis with preservation of the immediate–early gene response. *Surgery* 2002; **131**: 556–563.
28 Pratt DS, Kaplan MM. Evaluation of liver function. In *Harrison's Principles of Internal Medicine* (16th edn), Kasper DL, Fauci AS, Longo DL, Braunwald E, Hauser SL, Jameson JL (eds). McGraw-Hill: New York, 2005; 1813–1816.
29 Gujral JS, Liu J, Farhood A, Hinson JA, Jaeschke H. Functional importance of ICAM-1 in the mechanism of neutrophil-induced liver injury in bile duct-ligated mice. *Am J Physiol Gastrointest Liver Physiol* 2004; **286**: G499–G507.
30 Gujral JS, Farhood A, Bajt ML, Jaeschke H. Neutrophils aggravate acute liver injury during obstructive cholestasis in bile duct-ligated mice. *Hepatology* 2003; **38**: 355–363.
31 Gehring S, Dickson EM, San Martin ME, van Rooijen N, Papa EF, Harty MW *et al*. Kupffer cells abrogate cholestatic liver injury in mice. *Gastroenterology* 2006; **130**: 810–822.
32 Novobrantseva TI, Majeau GR, Amatucci A, Kogan S, Brenner I, Casola S *et al*. Attenuated liver fibrosis in the absence of B cells. *J Clin Invest* 2005; **115**: 3072–3082.
33 Wynn TA. Fibrotic disease and the T(H)1/T(H)2 paradigm. *Nat Rev Immunol* 2004; **4**: 583–594.
34 Kountouras J, Billing BH, Scheuer PJ. Prolonged bile duct obstruction: a new experimental model for cirrhosis in the rat. *Br J Exp Pathol* 1984; **65**: 305–311.